

# Effect of Temperature on the Optical and Electro-Optical Properties of Poly(methyl methacrylate)/E7 Polymer-Dispersed Liquid Crystal Composites

R. R. Deshmukh, M. K. Malik

Department of Physics, Institute of Chemical Technology, University of Mumbai, Matunga, Mumbai 400 019, India

Received 23 July 2007; accepted 29 December 2007

DOI 10.1002/app.27933

Published online 1 April 2008 in Wiley InterScience (www.interscience.wiley.com).

**ABSTRACT:** Experiments on the effect of temperature on the optical and electro-optical behaviors of polymer-dispersed liquid crystals (PDLCs) are considered. Composite films composed of poly(methyl methacrylate) (PMMA) and the nematic-type liquid crystal (LC) E7 were prepared by solvent casting in chloroform. The PDLC film contained droplets of E7 from 10 to 80 wt % in a PMMA matrix. Morphological studies illustrated the formation of isolated droplets of LC due to phase separation, and their homogeneous distribution increased with increasing E7 content. Thermo-optical studies showed an increase in the nematic-isotropic transition temperature of composites, which indicated preferential solvation during the phase-separation process. The electro-optical characteristics were studied under the conditions of an externally applied square wave

electric field with a He-Ne laser ( $\lambda = 632.8$  nm) as a light source. The responses improved as the E7 content in PMMA increased. Semipermanent memory effects were noticed in composites at higher temperatures. Changes in the transmittance due to thermal variations provided the possibility of using such a device as a temperature sensor. The results obtained indicate that under these experimental conditions, the output can be controlled to the desired level by the selection of a suitable loading of LC to prepare PDLC electro-optically active composite films with a response time on the order of only a few milliseconds. © 2008 Wiley Periodicals, Inc. *J Appl Polym Sci* 109: 627–637, 2008

**Key words:** PDLC; thin films; composites; electro-optical; electron microscopy

## INTRODUCTION

Polymer-dispersed liquid crystal (PDLC) films are relatively new composite materials that are currently revolutionizing liquid-crystal display technology because of their excellent electro-optical features.<sup>1–6</sup> They are also extremely useful for application in different domains of modern technology involving, for example, phase modulators,<sup>7,8</sup> variable attenuators,<sup>9</sup> polarizers,<sup>10</sup> light switches,<sup>11</sup> flexible displays,<sup>12</sup> and smart windows.<sup>13,14</sup> Recently, stressed liquid-crystal (LC) films consisting of interconnected LC domains dispersed inside stressed polymer matrices have been developed.<sup>15</sup> These composites produce a large electrically controlled phase shift and switch with submillisecond speed; the major applications of these new electro-optic materials are in high-speed displays, beam-steering devices, and light modulators.<sup>15–20</sup>

PDLC films are composed of LC droplets embedded in a polymeric matrix and are formed by the

phase separation of the LC component from a homogeneous solution with a polymer or prepolymer.<sup>21</sup> The film is then sandwiched between two glass slides with a transparent conductive substrate such as indium tin oxide (ITO). The resulting assembly forms an electrosensitive material that can be switched from a light-scattering state (off state) to a transparent state (the on state) by the application of an external electric field or thermal gradient.<sup>22–24</sup> These effects originate from the matching or mismatching of refractive indices between the LC droplets and polymer matrix. In the off state, surface anchoring causes a nonuniform director field within the droplets, and film scatters light because of the mismatching between the ordinary refractive index ( $n_o$ ) of LC and the polymer refractive index ( $n_p$ ). In the on state, the director is aligned along the field direction, and for normal light incident, the film becomes transparent if  $n_o = n_p$ .<sup>25–27</sup>

Three general methods have been developed for the formation of PDLCs:<sup>28</sup>

1. Polymerization-induced phase separation, in which LC is dissolved in the monomer, which is then polymerized photochemically or thermally.
2. Solvent-induced phase separation (SIPS), in which the LC and the polymer (thermoplastic) are dissolved in a common solvent to create a

Correspondence to: R. R. Deshmukh (rajedeshmukh@rediffmail.com).

Contract grant sponsor: Board of College and University Development (BCUD), University of Mumbai.

single phase. Evaporation of the solvent results in phase separation of LC droplets. One can tune the droplet size by controlling the rate of solvent evaporation.

3. Thermally induced phase separation, in which the LC and a thermoplastic polymer form a homogeneous solution above the melting point of the polymer. The phase separation occurs by the rapid cooling of the melt.

For such films to perform optimally, LC droplet size, shape, and distribution must be carefully controlled because not only morphology but also the electro-optical properties of the fabricated PDLC films depend on the preparation conditions and the phase-separation process.<sup>29</sup>

In this study, LC droplets were embedded in a poly(methyl methacrylate) (PMMA) matrix by the SIPS method, and the effect of temperature on the optical and electro-optical behavior of these PDLC cells is reported. The high scattering and switching of these cells strongly depended on the aggregation structure, which could be controlled by the solvent evaporation rate and LC ratio during the film preparation process.<sup>30,31</sup>

Our objective of the thermo-optical characterization of the PDLC material in this study was to examine light transmission as a function of temperature for different concentrations of LC in PMMA and to observe its effect on the clearing temperature of these films. This characterization suggests the possibility of using such a PDLC system as a temperature sensor in thermal devices. Furthermore, we made an attempt to study the temperature dependence of the transmission for these films, and the results show a decrease in the threshold voltage and driving voltage as the temperature increased. Possible reasons are discussed.

## EXPERIMENTAL

### Materials

The nematic LC used in this study was the eutectic mixture E7 [kindly provided by E. Merck (Darmstadt, Germany)], which contained 51 wt % 4-cyano-4'-*n*-pentyl-biphenyl, 25 wt % 4-cyano-4'-*n*-heptyl-biphenyl, 16 wt % 4-cyano-4'-*n*-oxyoctyl-biphenyl, and 8 wt % 4-cyano-4'-*n*-pentyl-*p*-terphenyl. E7 was thermotropic in nature; that is, it changed phase as the temperature was changed. Its nematic–isotropic transition temperature ( $T_{NI}$ ) was 61°C, and  $n_o$  was 1.5216.

PMMA was used as a polymer matrix with an  $n_p$  value of 1.4966 and a glass-transition temperature of 95°C.

### Preparation of the PDLC samples

In this study, PDLC films with different compositions (w/w %) of polymer and LC were prepared by the SIPS method.<sup>32,33</sup> We prepared a homogeneous solution of an appropriate amount of polymer (PMMA) and LC (E7) in chloroform (solvent) by spreading it on ITO-coated glass as a substrate at room temperature (25°C). The glass plate was kept floating on mercury to obtain a uniformly thick film. To make a PDLC cell, we used another ITO-coated glass plate for sandwiching the solidified polymer matrix containing isolated LC droplets. Film thickness was controlled with a poly(ethylene terephthalate) film (as a spacer) with a thickness of 18  $\mu\text{m}$ . The arrangement was heated in an oven at 85°C for good sandwiching.

Further processing was performed by a final annealing step, which involved the heating of all the PDLC films above 61°C ( $T_{NI}$  of E7) to redissolve the entire amount of LC present in the films and then cooling at a rate chosen to obtain the best optical contrast.<sup>34</sup> A sudden cooling generally results in films with very high scattering in the off state but with high threshold and driving voltages. In this case, a cooling rate of 0.5°C/min was used for all of the PDLC composite films. This combination of phase separation followed by thermal annealing adds flexibility and ease to production of commercial PDLC films. During the preparation, composite films with LC loading greater than 80% (w/w) showed poor adhesion to the substrate as the entire LC could not be contained in the micropores of PMMA; hence, they were not studied. Similar observations were reported by Miyamoto et al.<sup>30</sup>

### Morphology

The morphology of the films was studied with scanning electron microscopy (SEM; Philips-XL-30). LCs were first extracted in methanol (a nonsolvent for PMMA) at room temperature, and then, these films were dried overnight *in vacuo* before they were viewed under SEM.

### Experimental setup for the thermo-optical and electro-optical measurements

The electro-optic properties of the prepared PDLC cells were studied in terms of transmission changes with a driving alternating-current frequency. Variation in transmittance was measured for different frequencies between 50 Hz and 1 KHz. The experimental setup is given in Figure 1. A collimated beam of a He–Ne laser (wavelength = 632.8 nm) with 10 mW of power without any polarizer was used as an incident light source. The voltage was increased in

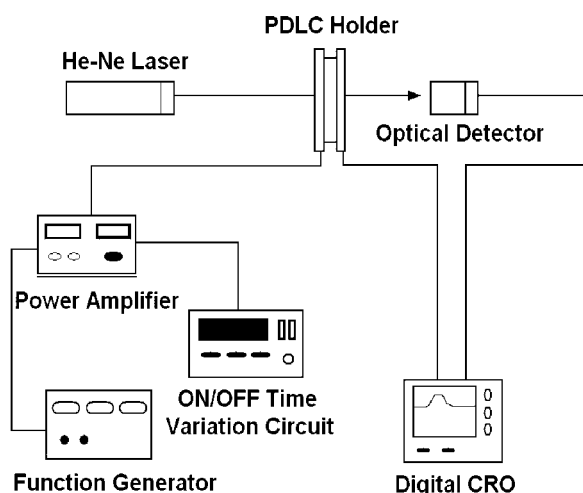


**Figure 1** Experimental setup for the thermo-optical and electro-optical measurements. CRO: Cathode Ray Oscilloscope.

steps of 10 V from 0 to 300 V during the scan-up cycle to drive PDLC cells and was decreased (scan-down cycle) in the same way to 0 V. Between all subsequent scan cycles, the PDLC films were kept for 5 min in the off state. The transmitted light intensity without any polarizer was measured in normal transmission geometry through a photodiode (Jain-Laser Tech, Mumbai, India). The distance between the PDLC cell and the photodiode was 300 mm. The response of the photodiode was monitored with a digital storage oscilloscope [Tektronix TDS 430A, 400 MHz (Beaverton, OR)].

We introduced an oven system in the same setup to measure the temperature dependence of transmission of these films. A temperature controller was used to control the temperature of the oven; it controlled the temperature to an accuracy of  $\pm 0.5^\circ\text{C}$  with a heating rate as low as  $0.5^\circ\text{C}/\text{min}$ . A heating rate of  $2^\circ\text{C}/\text{min}$  was used throughout this study. Furthermore, the actual sample temperature was continuously monitored by a PT-100 sensor (Best Engineering, Mumbai, India) close to the sample surface.

## RESULTS AND DISCUSSION

### Morphology

The degree of light scattering of composite films without an applied electric field greatly depends on their aggregation states. It is important to have LC domains of a size comparable to the wavelength of visible light ( $\sim 1\ \mu\text{m}$  or more) for strong light scattering. Another factor that greatly affects off-state transmission is the distribution of these LC domains. A high LC content will leave a small volume of the polymer unoccupied by phase-separated droplets,

which will thus efficiently increase light scattering. The most stable structure in the nematic phase is known by a uniform distribution of bipolar shaped droplets, but certain variations can rise due to restrictions of these droplets to spherical voids. These aggregation structures of LC droplets depend on their anchoring at the polymer-LC interface, types of LC and polymer used, their composition, their elastic properties, casting solvent, working temperature, rate of solvent evaporation, and so on.

In SIPS, the solvent evaporation rate plays a major role in the determination of the final aggregation structure of composite films. A fast evaporation rate of solvent will result in a considerable amount of LC residing in the polymer as an unseparated phase, which will result in the formation of small-size LC domains. A very slow evaporation rate will significantly increase the immiscibility between the polymer and LC to a great extent, which will thus allow the LC phase to separate efficiently and result in the formation of large LC domains.

Figure 2 shows the SEM micrographs of isolated E7 droplets in the PMMA matrix obtained after the extraction of E7 with methanol, which is a nonsolvent for PMMA. Clearly, there were no changes up to 20 wt % E7. Here, the LC components remained molecularly dissolved in the polymer matrix even after solvent evaporation, which suggests a lack of phase separation. Starting at 30 wt %, a homogeneous distribution of birefringent LC droplets was clearly identifiable where a phase-separation process took place after solvent evaporation. At LC concentrations greater than 30 wt %, the LC phase became continuous. In the composite films, PMMA formed three-dimensional spongy networks in which the phase-separated LC domains were embedded. Additionally, with increasing LC loading in the composites, the number of these LC structures formed out of a coalescing process of LC domains increased, which eventually led to the formation of continuous LC channels separated by walls of PMMA matrix. For 30–60 wt % LC, the shape of the isolated droplets was almost spherical; the droplets had a diameter of around 5–6  $\mu\text{m}$ . For composites with 70 wt % LC, few droplets were formed with a slightly elongated spherical morphology. The high-order elongation of the droplets in 80 wt % LC led to a bipolar shape. As discussed later, the larger size and bipolar shape of the LC droplets had a profound influence on the enhancement of the electro-optical performance by decreasing the threshold and switching voltages.

### Thermo-optical characteristics

Thermo-optical investigations provide us with the behavior of PDLC samples when they undergo temperature variation. To observe the temperature de-

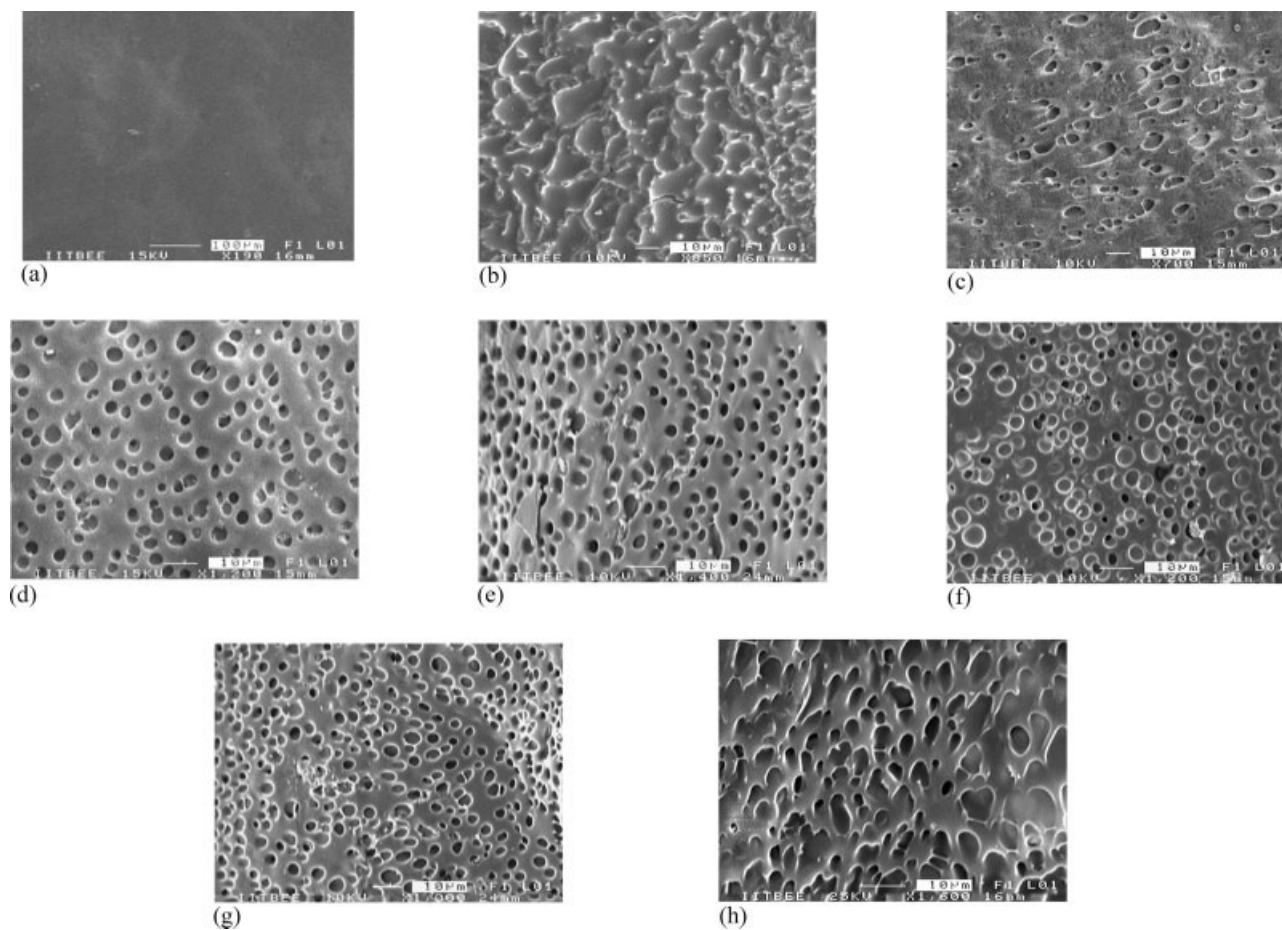


**Figure 2** SEM micrographs for the films with an LC droplet morphology: (a) 10, (b) 20, (c) 30, (d) 40, (e) 50, (f) 60, (g) 70, and (h) 80 wt % LC.

pendence of transmission, the temperature of the oven was changed from 25 to 100°C without the application of an external electric field. With increasing temperature, there was a decrease in the extraordinary refractive index of E7 along with a slight increase in  $n_o$ .<sup>35</sup> As a result, the effective refractive index ( $n_{eff}$ ) of LC decreased and came very close to  $n_p$ ; thus, transmittance increased. Figure 3 shows the percentage transmission change of the PDLC films as a function of temperature with various concentrations of E7 in PMMA. It was evident that at room temperature, transmission through the composite films increased as the LC concentration decreased, and the films had low optical contrast.

At low concentrations of LC (10 and 20%), light transmission at room temperature was very high and remained almost constant with increasing temperature. This was due to the fact that at this composition, the mixture of polymer and LC was a single phase i.e. a homogeneous system, even after solvent evaporation, and the film appeared to be optically isotropic [Fig. 2(a,b)]. For a concentration of 30 wt % LC, the transmission was slightly lower, which suggests the formation of LC droplets because of phase

separation [as shown earlier in Fig. 2(c)], and increased gradually to a maximum as the temperature increased.

The composites with LC content greater than or equal to 40 wt % showed a strong decrease in transmittance at room temperature. This was due to the

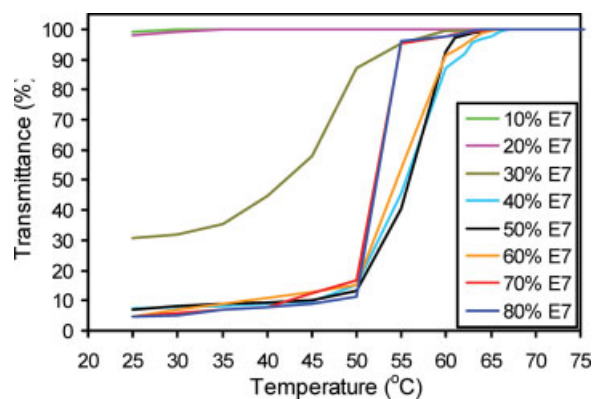


**Figure 3** Transmittance versus temperature for different weight percentages of E7. [Color figure can be viewed in the online issue, which is available at [www.interscience.wiley.com](http://www.interscience.wiley.com).]

homogeneous distribution of phase-separated LC droplets occupying a large part of the polymer matrix [Fig. 2(d–h)]. Their behavior with rising temperature was more striking when the transmittance remained practically constant up to a certain temperature and then increased rapidly. We call this temperature the *critical temperature*, which is defined as the temperature above which the transmission increases abruptly. A critical temperature value around 50°C was seen for all of the composites in this study. As shown in Figure 3, composites with 40–60 wt % E7 showed a clear switching effect in the temperature range 50–60°C. Furthermore, this response became more or less upright as the E7 content in PMMA increased. A steeper behavior was found with higher contents of E7 (70 and 80 wt %); this formed a thermal switch that could operate in a narrow range of 50–55°C.

Another consequence of thermo-optical behavior included a shift in the  $T_{NI}$  of these phase-separated systems compared to that of pure E7. A nematic–isotropic phase transition at temperatures higher than 61°C was found for the PMMA/E7 system in this study. When the temperature was raised to 61°C, the films became highly transparent, but there was still a marginal increase in transmitted light power as the temperature was further increased, which resulted in an increase in  $T_{NI}$ . This behavior may have been related to a preferential solvation of E7 constituents.<sup>36</sup> Figure 4 shows the dependence of  $T_{NI}$  of the PMMA/E7 composites on the LC concentration. Composites with a higher concentration of PMMA showed a higher increase in  $T_{NI}$  compared to the ones with lower PMMA contents.

The high transparent state of films beyond  $T_{NI}$  could not be related to the refractive index matching proposition, as there was still a considerable difference between the refractive index of both the polymer and LC.<sup>22</sup> The explanation for this fundamentally involves an analysis of the LC order parameter

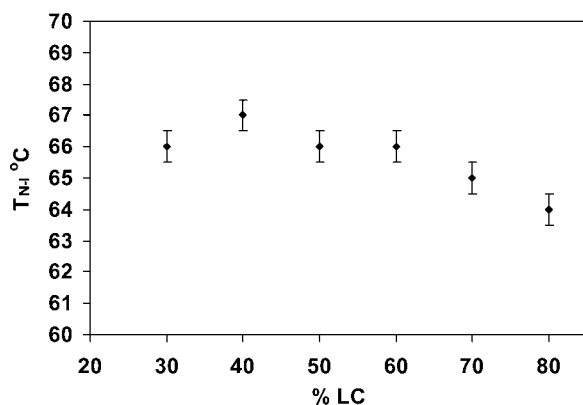


**Figure 4** Dependence of  $T_{NI}$  of the PMMA/E7 system as a function of the E7 concentration.

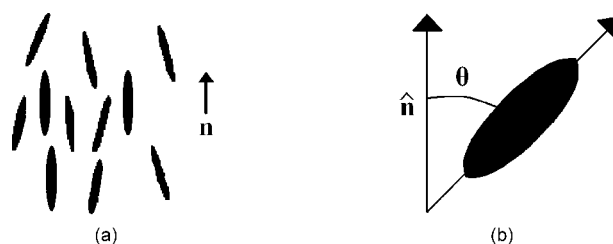


**Figure 5** (a) Alignment of molecules in an LC and (b) orientation of a single molecule with a local director ( $n$ ).

( $S$ ).  $S$  is a normalized parameter that indicates the degree of order of a system. Traditionally,  $S$  is given as

$$S = (1/2)(3 \cos^2 \theta - 1) \quad (1)$$

where  $\theta$  is the angle between the long axis of each molecule and the local director (which is the preferred direction in a LC sample), as shown in Figure 5. The brackets denote an average over all of the molecules in the sample.

For a completely random and isotropic sample (e.g., liquids),  $S = 0$ , whereas for a perfectly aligned sample (e.g., solids),  $S = 1$ . For a typical LC sample,  $S$  has a value of 0.3–0.8. This value generally decreases as the temperature is raised. In particular, a sharp drop of  $S$  to 0 is observed when a sample undergoes a phase transition from the nematic phase to the isotropic phase, where it has an appearance of a clear liquid.

Now, as the temperature of samples containing LC droplets is increased beyond  $T_{NI}$ , the transparent state arises due to the dissolution of the LC mixture (in clear liquid state now) in the polymer matrix and, hence, leaves no scattering sites.

### Effect of the LC concentration on the electro-optical properties

Figure 6 shows off-state and on-state (50 Hz, 200 Vp-p) transmission of PMMA films with various E7 contents measured at 25°C at which E7 was in the nematic state. The purpose of this experiment was to obtain optimized composite films that exhibited maximum optical contrast.

In the off state, composite films showed minimum value of transmittance with loadings of 40–80 wt % E7 in PMMA. For  $E7 \leq 40$  wt %, the transmittance was higher even without an applied electric field. At 30 wt % E7, although the phase-separation process yielded a considerable amount of isolated droplets in PMMA [Fig. 2(c)], a large portion of the polymer matrix was left undispersed and optically isotropic. The strong light intensity contrast (difference in the transmittance of the cell with and without applied

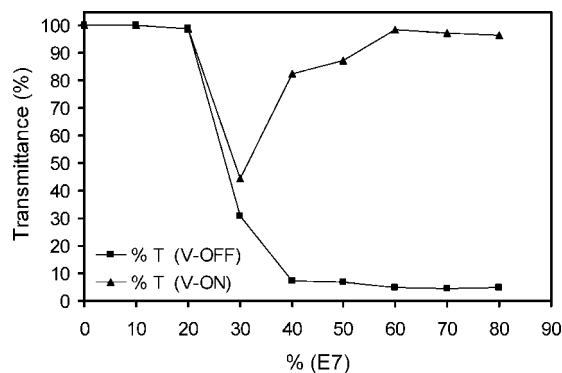


**Figure 6** Variation of the light transmittance through the PMMA/E7 composite films as a function of the E7 concentration under the conditions of a 50-Hz alternating-current field of 200 Vp-p at 25°C (V-OFF = voltage off; V-ON = voltage on).

electric field) appeared in the range 60–80 wt % E7. A dramatic decrease in the transmittance in the off state for films with E7 greater than or equal to 40 wt % indicated that the formation of continuous, three-dimensional LC channels (Fig. 2) was important for light scattering. Thus, we concluded that the switching from low transmittance in the off state to high transmittance in the on state for composite films with E7 loadings of 60–80 wt % makes them a promising candidate for electro-optic measurements.

### Electro-optical responses

To analyze the electro-optical behavior of our samples, we measured transmittance variation by changing the amplitude and frequency of the applied electric field. The applied field was driven by a square wave voltage with frequency varying from 50 Hz to 1 KHz, and we found that 200 Hz was the optimum frequency for our samples. The variation in transmittance at 200 Hz as a function of the applied electric field with different E7 concentrations at a normal viewing angle is shown in Figure 7.

The transmittance increased slightly with voltages up to 20 V and then increased rapidly in the range 20–60 V and reached saturation. We recorded the threshold voltage as  $V_{th}$  (the voltage for which the transmittance was 10% of the total transmittance change) and the switching voltage as  $V_{90}$  (the voltage for which the transmittance was 90% from the original transmission).

When the voltage applied to the samples was lower than  $V_{th}$ , very little alteration was induced on the LC molecular director. When the amplitude of the applied voltage was above  $V_{th}$ , the LC molecules started aligning themselves parallel to the electric field direction,<sup>37</sup> which thus reduced the mismatch between the refractive indices of the polymer matrix and the LC domains. A complete or maximum

matching of the refractive indices took place at higher voltages, where the light transmission achieved a maximum value. This voltage, known as the *driving voltage*, drove the PDLC cells from a minimum transmission ( $T_{min}$ ) to a maximum transmission ( $T_{max}$ ) and was different for different samples. The PDLC films composed of higher concentrations of polymer required higher threshold and switching voltages. The reason was that the polymer, as a typical dielectric material having a comparatively higher dielectric constant than that of LC, consumed a great part of the applied voltage, which thus led to a reduced effective voltage for LC. Another reason for the same behavior may be related to the LC droplet formation in the polymer matrix. If one considers the configuration and morphology of the E7 droplets (Fig. 2), it is interesting to see that although the average size of the droplets was almost same for composites having 70 and 80 wt % E7, the electro-optical properties were a little enhanced because of the bipolar shape of droplets for the latter, where a fast switching took place.

During the study of electro-optical properties, a well-known hysteresis phenomenon,<sup>2</sup> which indicated a lower transmission at a given voltage during the scan-up cycle as compared to the transmission at the same voltage during the scandown cycle, was observed in all of the electro-optic curves of our samples. Figure 8 shows the hysteresis effect of the PMMA/E7 composite films. A measure of hysteresis is given by the voltage width at half-maximum ( $\Delta V_{50}$ ). It has been suggested that hysteresis might be due to the possible defect movement in a droplet.<sup>2,38</sup> Reamy et al.<sup>38</sup> observed that hysteresis may be related to the mechanism of orientation of the droplet director, which ultimately may depend on the polymer/LC compatibility induced interfacial polymerization.

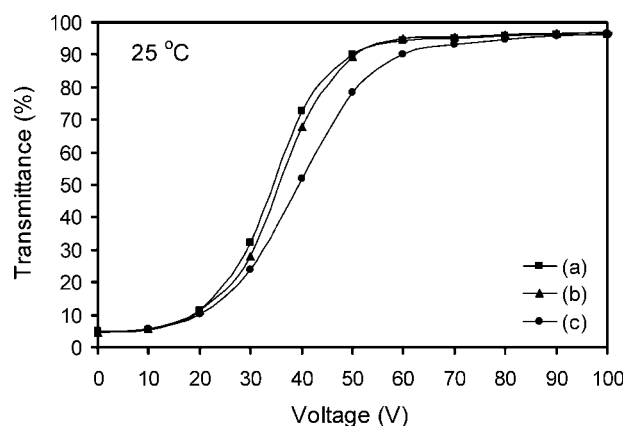


**Figure 7** Transmittance versus applied voltage for PMMA/E7: (a) 20/80, (b) 30/70, and (c) 40/60% (w/w) composite films at 200 Hz and 25°C.

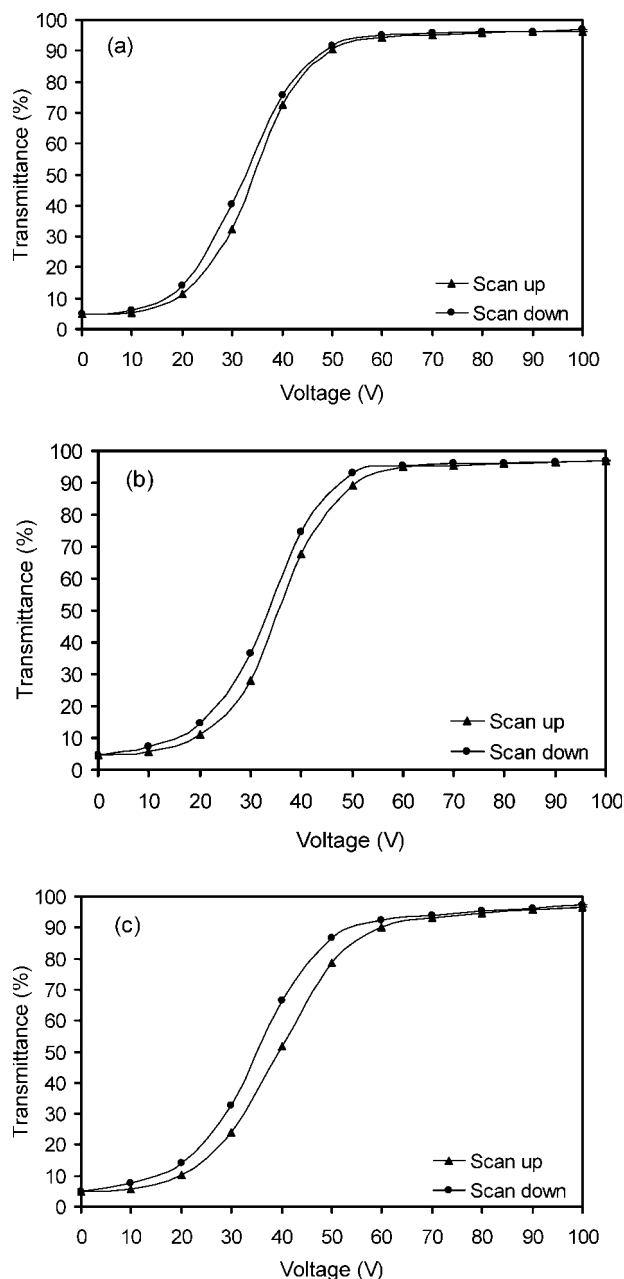


**Figure 8** Hysteresis curves of PMMA/E7: (a) 20/80, (b) 30/70, and (c) 40/60% (w/w) composites measured at 200 Hz.

We observed that  $\Delta V_{50}$  became less significant as the E7 content in PMMA increased. One possible reason might be related to the morphology of the LC droplets, as shown in Figure 2, where an increase in the LC concentration increased the size of the droplets formed out of the phase-separation process. As a result, the films with droplets of bigger sizes responded quickly to an applied field, as elucidated by Figure 7. This quick response during both scan cycles (up and down) reduced  $\Delta V_{50}$  efficiently. Hence, this clearly suggests that the formation of large bipolar droplets is necessary for the formation

of a PDLC device with good stability and electro-optical characteristics.

Next, we attempted to study the dependence of the light transmission on the applied field at various temperatures for these samples. The temperature was increased from 25 to 50°C in steps of 5°C. It was worth recording these characteristics at 50°C, where the off-state transmittance was comparatively very low as compared to the one at 55°C (Fig. 3). These voltage–transmittance curves as a function of temperature for films with different weight percentages of E7 are reported in Figure 9.

The threshold field and driving voltages decreased and the transmittance curves shifted to lower voltages with increasing temperature. The variation in  $V_{th}$  and  $V_{90}$  for the composites as a function of temperature is shown in Figure 10.  $V_{th}$  and  $V_{90}$  decreased with increasing temperature. This lowering of voltages can be easily understood as follows: when the temperature was increased, the order parameter of E7 decreased strongly. As a result, the solubility of E7 in PMMA increased, which increased the actual refractive index of PMMA slightly. In addition,  $n_{eff}$  of the nematic state approached a value very close to  $n_p$ . Thus, an applied field, even with small amplitude, reoriented the LC molecules sufficiently to satisfy the condition of refractive index matching, and hence, transmittance became a characteristic of lower voltages as the temperature increased.

The thermal hysteresis effects of composites are shown in Figure 11. Here we see that the hysteresis for these curves extended to zero field. The off-state transmittance after the scandown cycle did not return to its original scattering state, and the film retained some portion of the saturating transmittance even after the removal of the applied field. This phenomenon is known as *persistence*.<sup>28</sup> Unlike the memory effect, where a film is in a particular transmission state indefinitely or unless heated above  $T_{NI}$ , the film in persistence requires some time to relax to the original off state. In this study, all of the samples were characterized by relaxation times of a few minutes for applied fields above room temperature. This may have been due to the presence of polarization fields at higher temperatures, which aligned the LC molecules even after field removal. We can, therefore, argue that these experimental changes were due to a synergetic action of both the applied field and temperature. Nevertheless, the understanding of persistence in PDLCs needs careful study, as the relation between the electric field and temperature alone cannot justify the phenomenon. However, we feel that the *in situ* measurement of the electro-optical properties and LC droplet response with the help of a polarizing microscope would help us better in understanding the problem.

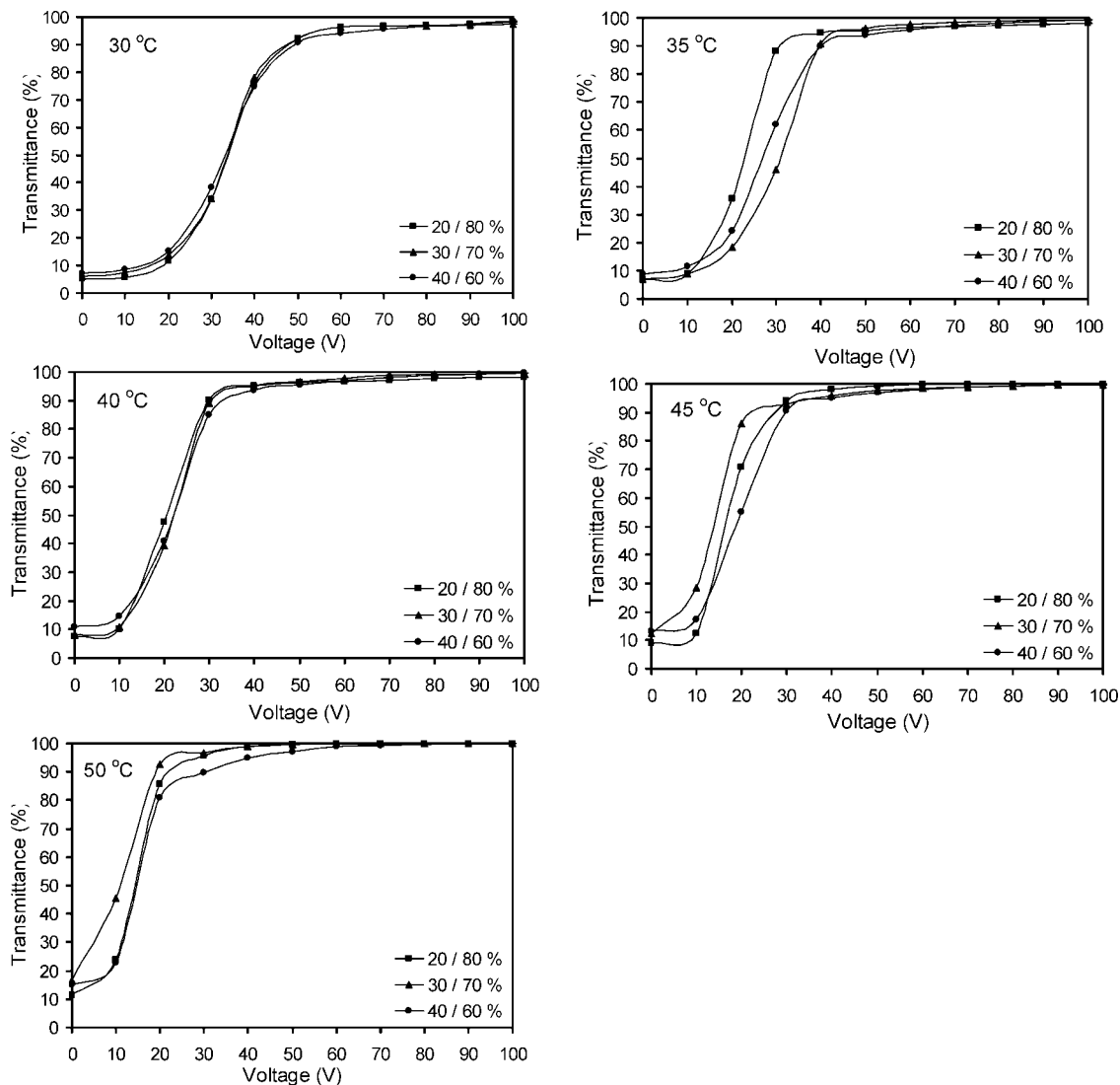


**Figure 9** Temperature-dependence transmission characteristics of the PDLC films for different PMMA/E7 weight percentages as a function of the applied voltage at 200 Hz.

In search of a material with a good quality of electro-optical response functions, one seeks composites with low  $V_{thr}$ ,  $V_{90}$ , and  $\Delta V_{50}$  and a high contrast ratio. An increase in temperature greatly reduced

the threshold and switching voltages of the samples. In addition, there was a decrease in the optical contrast of all of the samples, as shown in Figure 12. Hence, a decrease in  $V_{th}$  and  $V_{90}$  was insignificant at

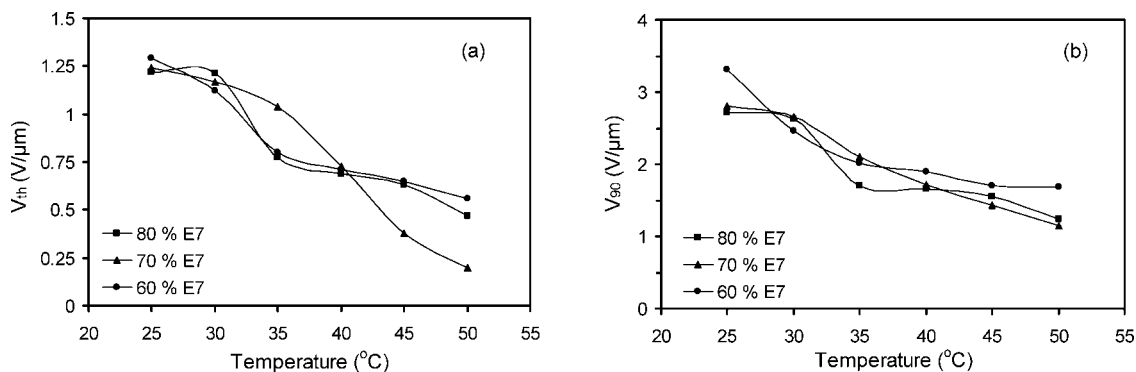


**Figure 10** Temperature dependence of (a)  $V_{th}$  and (b)  $V_{90}$  with various weight fractions of E7 in a PMMA matrix.



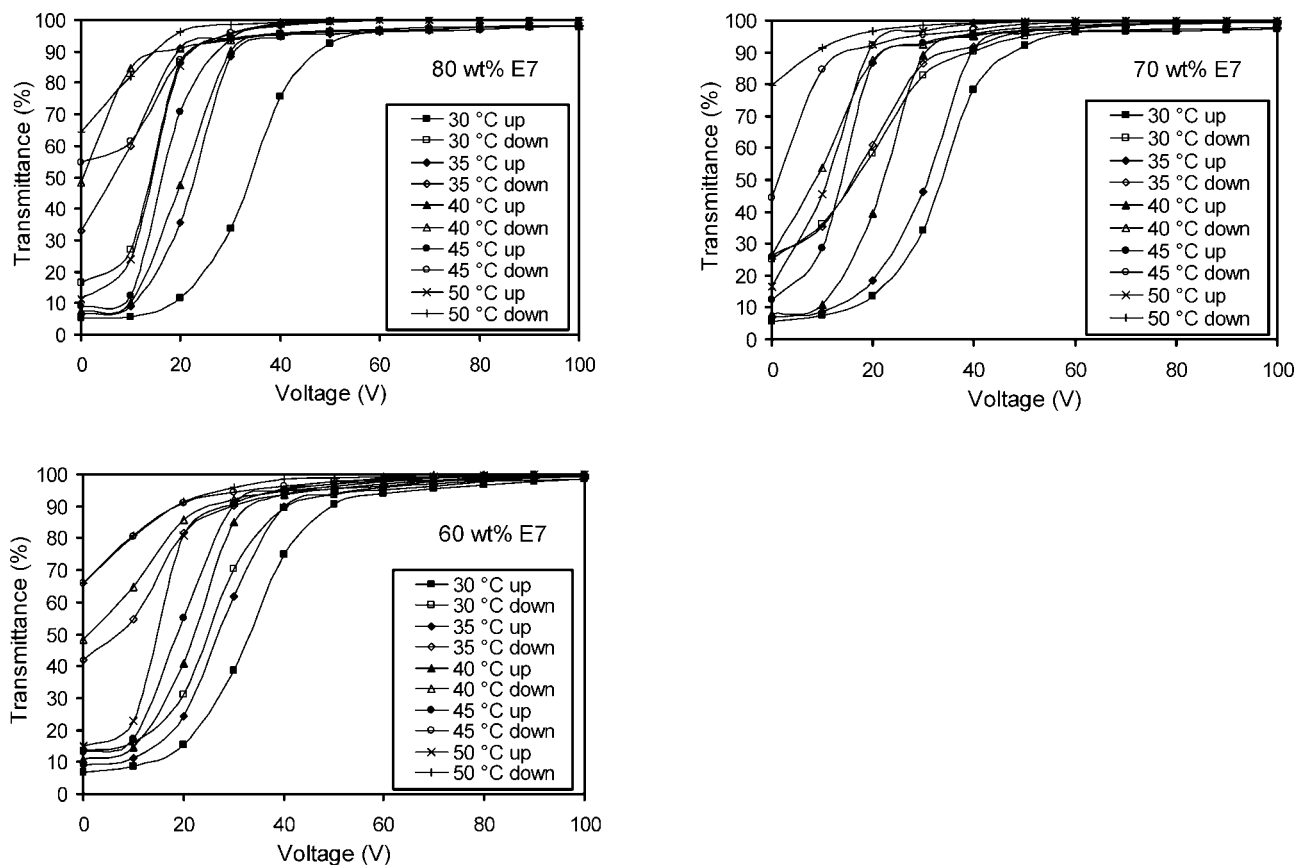


Figure 11 Plots of thermal hysteresis for PMMA/E7 composites with different E7 contents.

higher temperature values, where the transmittance in the off state was slightly high, which led to a noteworthy decrease in the optical contrast of all of the films.

Other criteria for evaluating the film performance is the time it takes to switch from an opaque to a transparent state and vice versa. This time is known as the *response time* (RT) of a film. We measured the switching responses of our samples as a function of both voltage and frequency. The responses were

very good when the voltage was greater than or equal to 40 V. The measurement results show that the fall time or decay time ( $\tau_D$ ) of our samples was very large compared to the rise time ( $\tau_R$ ).  $\tau_R$  is defined as the time required for the transmittance to change from 10 to 90% upon turn-on, and  $\tau_D$  is defined as the time required for the transmittance to change from 90 to 10% upon turn-off. Figure 13 shows  $\tau_R$  and  $\tau_D$  of the PDLC samples with various LC contents as a function of voltage.

$\tau_R$  can be continuously controlled with voltage because the magnitude of  $\tau_R$  is mainly a function of the applied field; on the other hand,  $\tau_D$  is not closely related to the magnitude of the applied voltage but to the viscosity and elasticity of LC molecules and to the interfacial interaction between the polymeric wall and LC molecules. The latter process is generally slower than the former, and hence,  $\tau_R$  is shorter than  $\tau_D$ . The large values of  $\tau_D$  in our samples may have been due to a residual electric charge, which served as a capacitor.

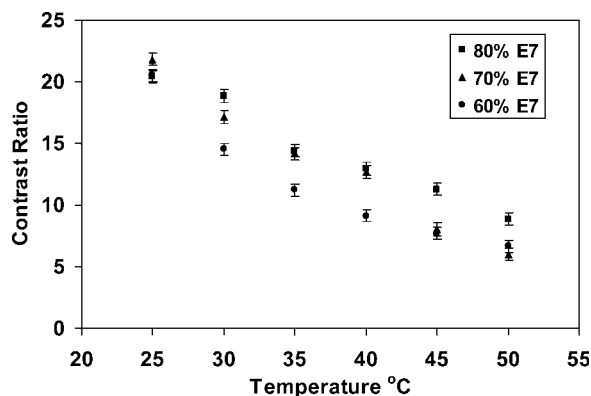
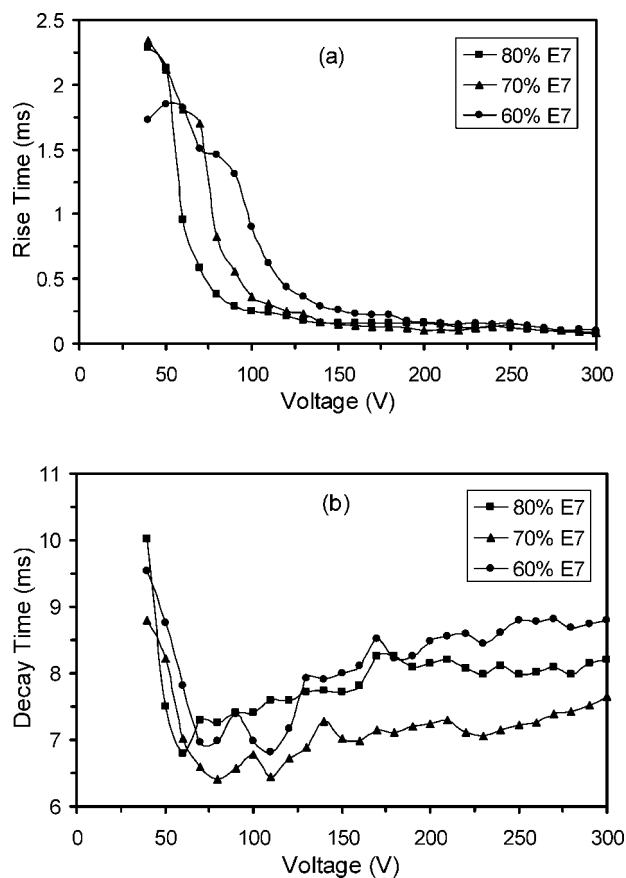


Figure 12 Contrast ratio of the PMMA/E7 PDLC films as a function of temperature.

## CONCLUSIONS

This article deals with a temperature-dependence study of the optical and electro-optical properties of



**Figure 13** Magnitude of (a) rise and (b) fall times as a function of voltage for the PMMA/E7 composite films with different E7 contents.

PDLC films with various LC contents in a polymer matrix. It was clear that the light transmittance strongly depended on the concentration of LC, where films with higher LC contents produced the best contrast. The morphology of these composite films has been discussed in this article. Above a particular concentration of LC, phase separation occurred. A three-dimensional spongy network of PMMA matrix contained the phase-separated LC domains, and their number increased with increasing LC content. Also, the average droplet size increased and there was a change in droplet morphology from spherical to high order elongation as the LC concentration in the host polymer increased. The formation of large, bipolar droplets was necessary for optimum responses from the PDLC films.

The results, obtained experimentally, suggest that the thermo-optical behavior of all of the composites showed a change in light transmission based on thermal variations. This performance can be used to realize temperature sensors. A  $T_{NI}$  higher than that of pure LC was found in all of our samples, which suggested preferential solvation during the phase-separation process.

The contrast ratio of the composite films selected for electro-optical measurements showed that these films exhibited low transmission in the off state and very high transmission in the on state. Films with higher loadings of LC showed good electro-optical responses. Furthermore, the threshold field and switching voltages dropped significantly as a consequence of increasing temperature. The response time observed was of the order of only a few milliseconds, which makes these composites useful for display applications where the fast switching of electro-optic response is required.

The authors thank A. K. Kalkar for helpful discussions and S. A. Bhamre for help in installing the experimental setup for the research work.

## References

1. Wu, B. G.; West, J. L.; Doane, J. W. *J Appl Phys* 1987, 62, 3925.
2. Drzaic, P. S. *Liq Cryst* 1988, 3, 1543.
3. Drzaic, P. S.; Muller, A. *Liq Cryst* 1989, 5, 1467.
4. Doane, J. W. In *Liquid Crystals: Applications and Uses*; Bahadur, B., Ed.; World Scientific: Singapore, 1990; Vol. 1.
5. Bowley, C. C.; Crawford, G. P. *Appl Phys Lett* 2000, 76, 2235.
6. Han, J. J. *Kor Phys Soc* 2006, 49, 1482.
7. Ren, H.; Lin, Y.-H.; Fan, Y.-H.; Wu, S. T. *Appl Phys Lett* 2005, 86, 141110.
8. Vicari, L. *J Appl Phys* 1997, 81, 6612.
9. Ramanitra, H.; Chanclou, P.; Vinouze, B.; Dupont, L. *Mol Cryst Liq Cryst* 2003, 404, 57.
10. Baek, S.; Jeong, Y.; Kim, H.-R.; Lee, S.-D.; Lee, B. *Appl Opt* 2003, 42, 5033.
11. Lin, Y.-H.; Ren, H.; Wu, S. T. *Appl Phys Lett* 2004, 84, 4083.
12. Buyuktanir, E. A.; Glushchenko, A.; Wall, B.; West, J. L. *Proc SID* 2005, 1778.
13. Liu, J.; Wu, F. *J Appl Polym Sci* 2005, 97, 721.
14. Maschke, U.; Coqueret, X.; Benmouna, M. *Macromol Rapid Commun* 2002, 23, 159.
15. West, J. L.; Zhang, G.; Glushchenko, A. *SID Dig* 2003, 55, 1.
16. West, J. L.; Zhang, K.; Zhang, M.; Buyuktanir, E.; Glushchenko, A. *Proc SPIE* 2005, 59360 L, 5936.
17. Fulghum, J. E.; Su, L.; Artyushkova, K.; West, J. L.; Reznikov, R. *Mol Cryst Liq Cryst* 2004, 412, 361.
18. Zhang, G.; West, J. L.; Glushchenko, A.; Smalyukh, I. I.; Laverentovich, O. *Proc SID* 2005, p 691.
19. West, J. L.; Zhang, K.; Zhang, M.; Aoki, T.; Glushchenko, A. *Proc SPIE* 2005, 10, 5741.
20. Golovin, A. B.; Shiyankovskii, S. V.; Laverentovich, O. D. *Appl Phys* 2003, 83, 3864.
21. Khoo, I. C.; Wu, S. T. *Optics and Nonlinear Optics of Liquid Crystals*; World Scientific: Singapore, 1993.
22. Ren, Y.; Petti, L.; Mormille, P.; Blau, W. J. *J Mod Optics* 2001, 48, 1099.
23. Petti, L.; Mormille, P.; Blau, W. J. *Mol Cryst Liq Cryst* 2001, 359, 53.
24. Kayacan, O.; San, S. E.; Okutan, M. *Physica A* 2007, 377, 523.
25. Yang, D. K.; Chien, L. C.; Doane, J. W. *Appl Phys Lett* 1992, 60, 3102.
26. Jain, S. C.; Thakur, R. S.; Lakshmikummar, S. T. *J Appl Phys* 1993, 73, 1057.

27. Whitehead, J. B.; Zumer, S.; Doane, J. W. *J Appl Phys* 1993, 73, 1057.
28. Drzaic, P. S. *Liquid Crystal Dispersions*; World Scientific: Singapore, 1995.
29. Montgomery, G. P., Jr.; West, J. L.; Tamura-Lis, W. *J Appl Phys* 1991, 69, 1605.
30. Kajiyama, T.; Park, K.; Usui, H.; Kikuchi, H.; Takahara, A. *Proc SPIE* 1993, 122, 1911.
31. Park, K.; Kikuchi, H.; Kajiyama, T. *Polym J* 1994, 26, 895.
32. Kajiyama, T.; Miyamoto, A.; Kikuchi, H.; Morimura, Y. *Chem Lett* 1989, 813.
33. Kim, B. K.; Ok, Y. S. *J Appl Polym Sci* 1993, 49, 1769.
34. Mucha, M. *Prog Polym Sci* 2003, 28, 837.
35. Alkeskjold, T. T.; Laegsgaard, J.; Bjarkley, A.; Hermann, D. S.; Anawati; Broeng, J.; Li, J.; Wu, S. T. *Opt Express* 2004, 12, 5857.
36. Bedjaoui, L.; Gogibus, N.; Ewen, B.; Pakula, T.; Conqueret, X.; Benmouna, M.; Maschke, U. *Polymer* 2004, 45, 6555.
37. Pankaj, K.; Raina, K. K. *Curr Appl Phys* 2007, 7, 636.
38. Reamey, R. H.; Montoya, W.; Wong, A. *Proc SPIE* 1992, 2, 1665.